

Article

Evaluating the Influence of Waste Cooking Oil Molecular Structure on Aged Asphalt Modification

Qiu hao Chang ^{1,*}, Liang liang Huang ^{2,*}  and Yuting Wu ³

¹ The Department of Civil and Natural Resources Engineering, University of Canterbury, Christchurch 8140, New Zealand

² School of Sustainable Chemical, Biological & Materials Engineering, The University of Oklahoma, Norman, OK 73019, USA

³ Department of Electrical & Computer Engineering, University of Wisconsin-Madison, Madison, WI 53706, USA; wu247@wisc.edu

* Correspondence: qiu hao.chang@canterbury.ac.nz (Q.C.); hll@ou.edu (L.H.)

Abstract: Recycling aged asphalt pavement has become increasingly important due to its environmental and economic advantages. Asphalt, serving as the binding agent for aggregates, plays a crucial role in pavement integrity. The deterioration of asphalt binder properties upon aging poses a significant challenge to asphalt pavement recycling. Consequently, various rejuvenators have been developed to restore aged asphalt binder properties and facilitate pavement reclamation. Waste cooking oil (WCO) is a widely used rejuvenator that mitigates the high viscosity and brittleness of aged asphalt, preventing cracking. WCO consists of triglycerides (TG) and free fatty acids (FFA), each with distinct molecular structures. In this study, molecular dynamics simulations were employed to investigate the individual effects of 10 wt.% TG and FFA on the viscosity, self-diffusion, and microstructure of aged asphalt at 1 atm and 404 K. The results demonstrate that both TG and FFA can reduce the viscosity of aged asphalt, albeit through different mechanisms. TG and FFA, characterized by high molecular mobility when dispersed in aged asphalt, enhance its mobility and reduce its viscosity. Additionally, TG effectively disrupts preferential interactions among asphaltenes, preventing their self-aggregation. In contrast, FFA has a limited impact on reducing these interactions. Furthermore, the study delves into the entanglement behaviors of FFA and TG with varying chain lengths within aged asphalt. Shorter chain lengths, as opposed to longer ones, exhibit a lower likelihood of entanglement with other asphalt molecules, resulting in increased molecular mobility and reduced asphalt viscosity. The fundamental insights gained from this research serve as a valuable reference for the application of waste cooking oil in the recycling of aged asphalt pavement. By shedding light on underlying molecular dynamics, this study contributes to the development of more effective and sustainable approaches to asphalt recycling.

Keywords: asphalt pavement recycling; asphalt binder; waste cooking oil; molecular dynamics simulation



Citation: Chang, Q.; Huang, L.; Wu, Y. Evaluating the Influence of Waste Cooking Oil Molecular Structure on Aged Asphalt Modification. *Constr. Mater.* **2023**, *3*, 543–557. <https://doi.org/10.3390/constrmater3040034>

Received: 26 October 2023

Revised: 29 November 2023

Accepted: 5 December 2023

Published: 6 December 2023



Copyright: © 2023 by the authors. Licensee MDPI, Basel, Switzerland. This article is an open access article distributed under the terms and conditions of the Creative Commons Attribution (CC BY) license (<https://creativecommons.org/licenses/by/4.0/>).

1. Introduction

Asphalt, a high-viscosity product derived from petroleum distillation, serves as the essential binding agent for holding together aggregates or rocks in pavement construction. Over time, prolonged exposure to the elements leads to the oxidation and localized weathering of asphalt, resulting in the degradation of its properties. This deterioration ultimately impairs the functionality of asphalt binders in pavement structures. The restoration of aged asphalt binder properties is a pivotal step in facilitating the reclamation of asphalt pavement, offering substantial environmental and economic advantages. Notably, asphalt pavement comprises over 90% of the road infrastructure in the United States. It is estimated that the reclamation of asphalt pavement saves approximately USD 2.5 billion annually in

the U.S. [1]. This highlights the significance of rejuvenating aged asphalt to extend the life of pavement infrastructure while delivering cost savings and reducing environmental impact.

Various technologies are being developed to restore the diverse properties of aged asphalt binder and facilitate its re-utilization. Viscosity, a critical rheological property of asphalt, directly impacts its hardness and resistance to cracking [2]. Oxidation processes significantly elevate the viscosity of asphalt binder, making it harder, reducing its resistance to rutting, and increasing the likelihood of cracking [3–6]. Waste cooking oil (WCO) has emerged as an effective solution for softening aged asphalt, as demonstrated through both experimental studies and computer simulations [7,8]. For instance, Zargar et al. [9] conducted experiments in which they blended different quantities of WCO with 40/50 aged asphalt at 408 K, revealing a reduction in asphalt viscosity with increasing WCO content. Similar experimental findings were reported by Ji et al. [10] at the same temperature. The viscosity of aged asphalt decreased as greater amounts of waste corn and soybean oil were incorporated into the mix. It is worth noting that the viscosity reduction effect became less pronounced when WCO concentrations exceeded 8 wt.%. Cao et al. [11] conducted experiments to assess the viscosities of aged asphalt mixed with varying doses of waste vegetable oil (WVO). They observed a linear decrease in the viscosity of aged asphalt as the dosage of WVO increased over a temperature range from 363 to 453 K. Furthermore, Gökalp and Volkan [12] reported that WCO, when used as an anti-aging agent for asphalt, effectively mitigated the aging-related effects on physical and rheological properties, including the viscosity, rutting factor, and softening point. These research findings underscore the promising role of waste cooking oil in rejuvenating aged asphalt binder, enhancing its properties, and ultimately promoting the sustainable reuse of asphalt in various applications.

Molecular dynamics (MD) computer simulations have been instrumental in scrutinizing the impact of WCO on asphalt properties at the molecular level. For example, Sonibare et al. [13] conducted simulations in which they augmented virgin asphalt with waste vegetable oils (WVOs) containing free fatty acids like linoleic, palmitic, and oleic acids at various temperatures. They observed a reduction in the viscosity of virgin asphalt when additional WVOs were introduced, and this viscosity-lowering effect was particularly noticeable at lower temperatures. Additionally, they found that WVOs facilitated a more homogeneous packing of components within the asphalt. In another study, Li et al. [14] employed WCO composed of free fatty acids, including hexadecenoic, stearic, and oleic acids, and discovered that these free fatty acids reduced the viscosity of aged asphalt while enhancing the cohesive interactions between molecules in the aged asphalt conducted at 298 K. In contrast, Qu et al. [15] investigated the introduction of triglycerides, a key component of WCO, into virgin asphalt and observed a decrease in the intermolecular cohesive interactions of virgin asphalt, consequently reducing asphalt viscosity. Furthermore, Chang et al. [16] explored the influence of 10 wt.% triglycerides on the viscosity and microstructure of aged asphalt at 404 K, employing a newly developed aged asphalt model. Their findings revealed that triglycerides reduced the viscosity of aged asphalt by weakening the interactions and aggregations formed between asphaltene molecules in aged asphalt. These MD simulations provide valuable insights into the molecular mechanisms underlying the impact of WCO components on asphalt properties, shedding light on the intricate dynamics at play in asphalt rejuvenation processes.

Triglyceride (TG), a predominant component found in most common edible oils [15], consists of a glycerol backbone linked to three fatty acids (FAs). Under certain cooking conditions, such as during frying activities, these fatty acids can separate from the glycerol backbone, becoming free fatty acids (FFAs) [17]. Previous studies [9,10,14–16] have demonstrated that both FFAs and TG possess the capacity to modify the viscosity of and soften aged asphalt. However, the specific influence of the structural disparities between TG and FFAs on aged asphalt modification has not received comprehensive attention. Moreover, the chain length of fatty acids within TG or FFAs can range from 6 carbons to 24 carbons, varying between different cooking oils [18,19]. For example, coconut oil comprises more

than 40 wt.% of FAs with a chain length of 12 carbons, while corn oil contains only 0.1 wt.% of 12-carbon FAs but exceeds 50 wt.% of FAs with an 18-carbon chain [17]. These variations in the molecular structure and chain length of waste cooking oil have not been extensively investigated regarding their impact on viscosity modification in aged asphalt. This research gap highlights the importance of understanding how these factors affect the selection and application of WCO as rejuvenators in asphalt modification.

In this study, MD simulations were employed to examine the influence of four distinct components from waste cooking oil on the viscosity of aged asphalt. These components encompassed two types of triglycerides (TGs) with varying chain lengths, one with a short chain of 13 carbons and another with a longer chain of 22 carbons, as well as two forms of free fatty acids (FFAs) with chain lengths matching the aforementioned TG variants, 13 carbons for short and 22 carbons for long. Furthermore, the study delved into the microstructure, molecular mobility, and molecular entanglement behaviors of WCO-modified asphalt to uncover the fundamental mechanisms at play. The subsequent sections of this paper are structured as follows: Section 2 provides insights into the construction of asphalt models and a detailed overview of the MD simulation process. Section 3 outlines the methodologies for computing asphalt properties and presents the corresponding results. Finally, Section 4 offers the conclusions drawn from the findings of this study.

2. Asphalt Models and Simulation Details

MD simulation is a powerful computational tool that allows researchers to study the interactions and behaviors of numerous particles within a specific system. It is firmly rooted in the principles of statistical mechanics and thermodynamics. By applying Newton's laws, MD simulations enable the tracking of interaction forces, particle velocities, and positions within a system over time. This continuous updating of particle properties results in the time evolution of the entire system, often referred to as the system's trajectory. The trajectory generated by MD simulations provides a means to investigate both the static and dynamic properties of the system at the molecular level. Moreover, these simulations can compute a wide range of macroscopic physical properties. MD simulations offer distinct advantages, particularly in situations in which experimental replication would be challenging or impossible, such as ultra-high pressure and temperature conditions [20–23], studies of fluid confinement behavior [24–26], investigations at the nanoscale interface [27–30], and examinations of complex molecular interactions [31–33].

In recent years, MD simulations have emerged as a valuable tool for studying asphalt and its modifications [34,35], particularly at the molecular level, providing fundamental insights. Asphalt composition can be classified into four main categories based on the SARA fractions theory [36], which stands for saturates (S), aromatics (A), resins (R), and asphaltenes (A). To facilitate MD simulations in asphalt research, molecular models have been developed for each fraction. The left side of Figure 1 illustrates models of virgin asphalt molecules proposed by Zhang and Greenfield [37], Li and Greenfield [38], and Wang et al. [39]. These models have served as the basis for conducting MD simulations to explore the properties of virgin asphalt. Following the oxidation of asphalt, researchers have identified six oxygen-containing functional groups as oxidative products, including ketones, sulfoxides, anhydrides, carboxylic acids, alcohols, and polynuclear aromatics [40]. To align with the chemistry of asphalt oxidation, Chang et al. [16] introduced these six oxygen-containing functional groups to virgin asphalt models, leading to the development of a new model for aged asphalt, depicted on the right side of Figure 1. Saturates, typically characterized by low chemical reactivity, exhibit strong resistance to air oxidation [4,40]. Consequently, no oxidation was considered for the saturate molecules in their aged asphalt model. By adjusting the number of molecules from both virgin and aged asphalt models, Chang and colleagues constructed an aged asphalt sample with a composition of 17% saturates, 36% aromatics, 33% resins, and 14% asphaltenes. In addition, the concentration of each functional group in this sample is 0.60 mol/L for ketone, 0.27 mol/L for sulfoxide, 0.023 mol/L for anhydride, and 0.0068 mol/L for carboxylic acid, consistent with the

aged asphalts under 5 years of service. This asphalt sample has been rigorously validated for reliability and served as a reference sample in various studies, including the research described in this paper. For further details regarding the aged asphalt sample, readers are encouraged to refer to the cited paper by Chang et al. [16].

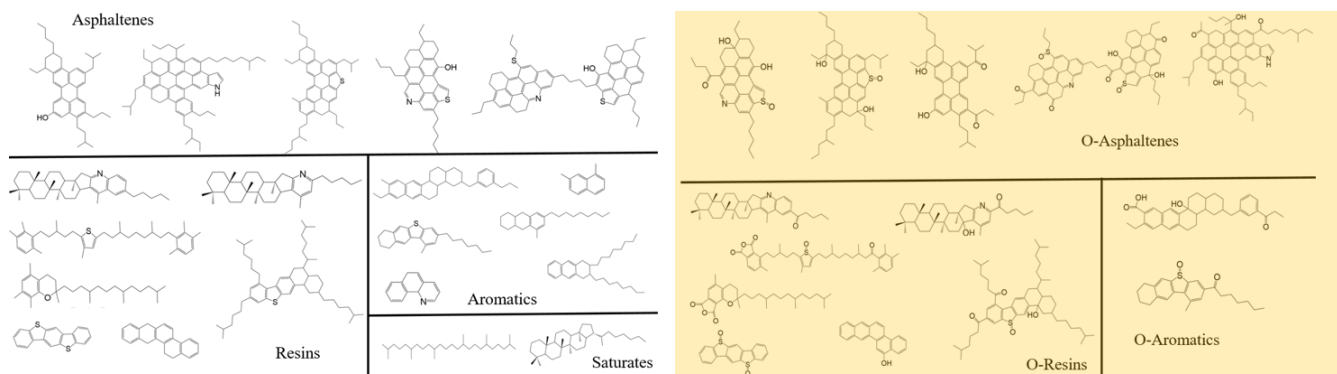


Figure 1. Left: Virgin asphalt models developed by Zhang and Greenfield [37], Li and Greenfield [38], and Wang et al. [39]. Right: Aged asphalt model developed by Chang et al. [16].

To investigate the effect of WCO molecular structure on the properties of aged asphalt, 10 wt.% WCOs with four different structures were mixed with aged asphalt separately at their blending temperature of 404 K [41,42]. Type I was a TG with a short chain length of 13 carbons, simply named TG13. Type II was a TG with a long chain length of 22 carbons (TG22). Type III was an FFA with a short chain length of 13 carbons (FFA13) and Type IV was an FFA with a long chain length of 22 carbons (FFA22). The molecular structure of each WCO component is shown in Figure 2.

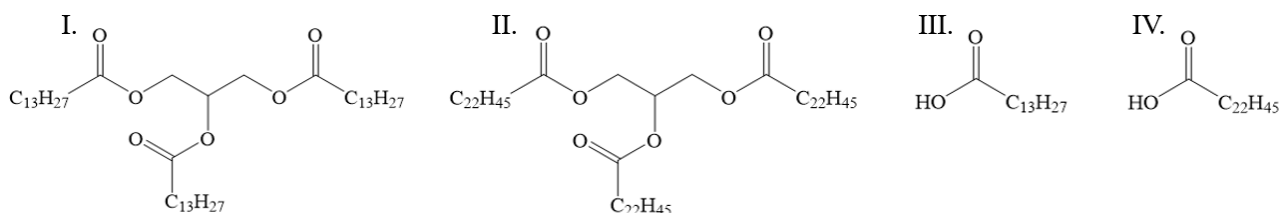


Figure 2. Molecular structures of TG13, TG22, FFA13, and FFA22.

Molecular dynamics simulations were carried out using the Large-scale Atomic/Molecular Massively Parallel Simulator (LAMMPS) [43]. Interactions within asphalt and WCO molecules were modeled using the OPLS-AA force field and a specific force field based on Paulina et al.'s work [44–48], respectively. For the non-bonded interaction calculations, a cutoff distance was set at 15 Å, and the Particle–Particle–Particle–Mesh (PPPM) method was employed for long-range electrostatic interactions. Initially, all molecules were positioned randomly in a cubic simulation box with a 20 nm edge using PACKMOL software [49], with periodic boundary conditions in all three dimensions (X, Y, and Z). The simulations began with a 1 ns canonical ensemble (NVT) at 404 K to energy-minimize the system. This was followed by a 20 ns isothermal–isobaric ensemble (NPT) at the same temperature and 1 atm pressure to achieve equilibrium. Post-equilibration, we collected the data for subsequent analysis. Figure 3 illustrates the initial configurations of the aged and WCO-modified asphalt simulations.

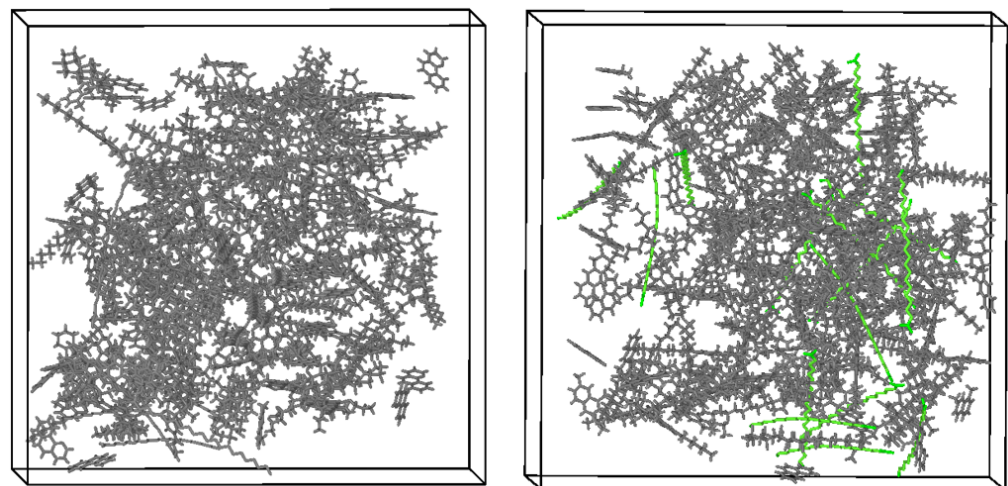


Figure 3. Left: Configuration of aged asphalt. Right: Configuration of WCO-modified asphalt (FFA22-modified asphalt as an example). Grey: asphalt molecules; green: FFA22 molecules.

3. Results and Discussions

3.1. Shear Viscosity

The Green–Kubo method, a typical method from MD simulations for computing asphalt viscosity, was used to determine the zero-shear viscosities of the aged and WCO-modified asphalts in this study [13,50–53]. Zero-shear viscosity is measured in shear deformation at a shear rate approaching to zero, which could be an indicator of the stiffness and rutting behavior of an asphalt binder. For example, it was found that zero-shear viscosity has a positive proportional relationship with the complex modulus, G^* , and is inversely proportional to the sine function of the phase angle, δ [54]. The zero-shear viscosity is derived through the integral of the pressure-tensor autocorrelation function over a correlation length

$$\mu = \frac{V}{kT} \int_0^{\infty} \langle P_{ij}^S(0)P_{ij}^S(t) \rangle dt \quad (1)$$

where P_{ij}^S is the off-diagonal pressure tensor of an element ij , V is the volume of the simulation system, T is the temperature, k is the Boltzmann constant, t is the time, and the angle bracket indicates the ensemble average.

The shear viscosities of the aged and WCO-modified asphalts at 1 atm and 404 K are shown in Figure 4. Before the modification, the aged asphalt had the highest viscosity, around 12 cP, which agrees well with the reference results under similar P/T conditions [13,55]. Introducing the WCOs into the aged asphalt clearly decreased its shear viscosity, consistent with the previous experimental observations [17]. It can be seen that the FFAs generally decreased the viscosity of the aged asphalt more than the TGs. In addition, considering the FFAs and TGs separately, the viscosity reduction in the aged asphalt with TG13 is obviously stronger than that with TG22, while the strength of the viscosity reduction from FFA13 and FFA22 in aged asphalt is almost the same. This observation indicates that the chain-length effect on the viscosity modification of aged asphalt exists in TGs but not considerably in FFAs.

3.2. Radial Distribution Function

The radial distribution function (RDF) was used to study the effects of WCOs on the microstructure of aged asphalt, understanding the fundamental mechanism of viscosity modification. The asphaltene fraction with the heaviest MW and the highest viscosity significantly affects the viscosity of asphalt. For example, it was reported that asphalt viscosity relates to the aggregations formed between asphaltenes in asphalt [56,57]. The strong aggregations formed between asphaltenes yield large-size asphaltene clusters in

aged asphalt and result in its high viscosity. By computing the RDF between asphaltene and asphaltene molecules, one can clearly show how these molecules are packed or aggregated in aged and WCO-modified asphalts. The RDF is defined as the normalized probability of finding particles at a distance r away from reference particles, shown as [50]

$$g(r) = \lim_{dr \rightarrow 0} \frac{\rho(r)}{4\pi\rho_{bulk}r^2dr} \quad (2)$$

where $g(r)$ represents the RDF between particle pairs, $\rho(r)$ is the local density of particle pairs between distances r and $r + dr$, and ρ_{bulk} indicates the bulk density of particle pairs in the simulation box. It is worth noting that $g(r)$ provides insight into the spatial distribution of particles within a system, effectively describing how particle density varies with distance from a point. This can reveal structural organization within a material at the molecular level, such as the propensity for clustering or uniform dispersion, which is critical for understanding the properties of the system being studied.

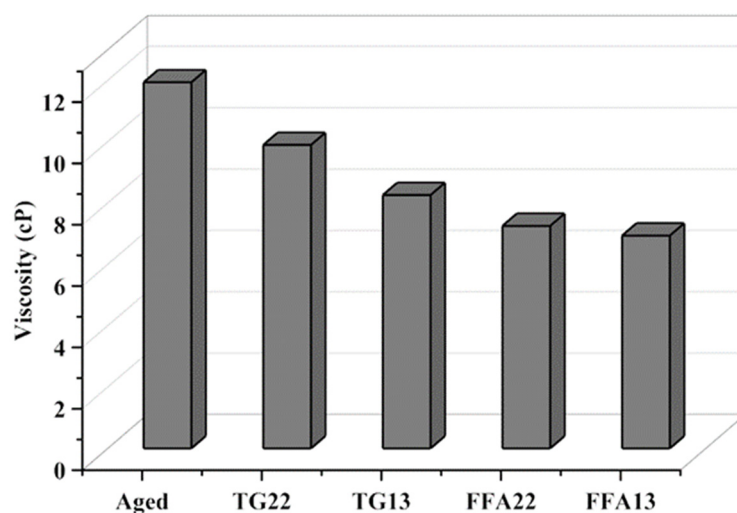


Figure 4. Shear viscosities of aged and WCO-modified asphalts.

The RDF results of the asphaltene–asphaltene pair of aged and WCO-modified asphalts are shown in Figure 5. The RDF of an asphaltene–asphaltene pair in aged asphalt has a first peak around 4 Å, indicating the preferential interactions among asphaltene molecules in the aged asphalt. The observation of such preferential interactions existing between asphaltenes in asphalt was reported in other publications before [58,59], which gave us confidence regarding the reliability of our RDF analysis. On the left of Figure 5, the peaks of the RDFs of the asphaltene–asphaltene pairs of TG13-modified and TG22-modified asphalts decreased, indicating that the TG molecules weakened the preferential interactions between the asphaltene molecules and could prevent their self-aggregation. In addition, the RDF of the asphaltene–asphaltene pair of the TG13-modified asphalt had a lower peak than that of the TG22-modified asphalt, suggesting that TG13 molecules could weaken the preferential interactions between asphaltenes more efficiently than TG22 molecules, which was probably the reason why TG13 had a stronger viscosity reduction effect on aged asphalt than TG22, as shown in Figure 4. On the right of Figure 5, the peaks of the RDFs of asphaltene–asphaltene pairs of FFA22-modified and FFA13-modified asphalts were similar to that of aged asphalt, indicating the FFA molecules did not obviously weaken the preferential interactions between asphaltenes and prevent their self-aggregation. Comparing the molecular structures of TG and a FFA, the glycerol backbone of the TG molecule has heteroatoms like oxygens that may enhance the interaction between an asphaltene molecule and itself, which is the possible reason for why the TG could weaken the interaction between asphaltenes but the FFA could not.

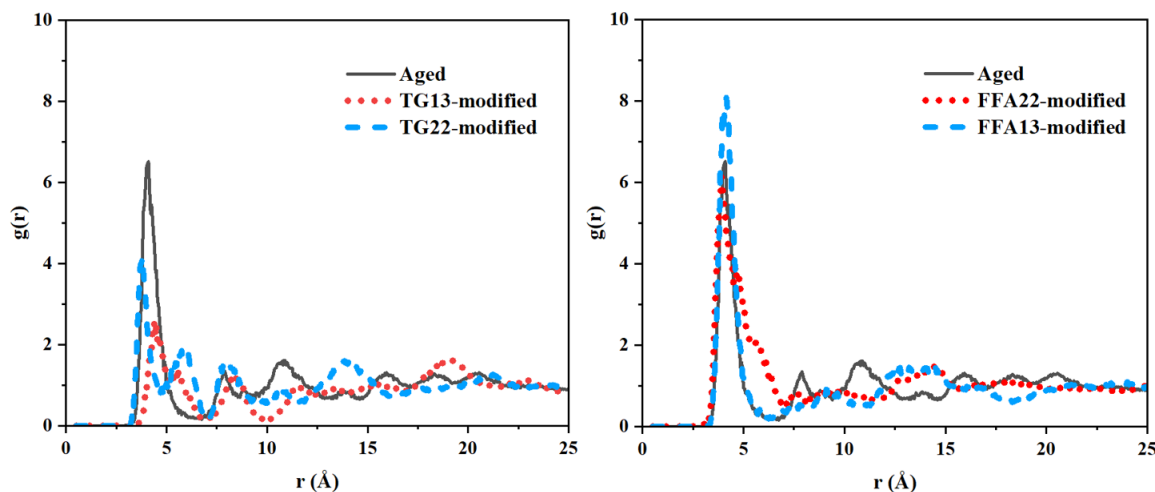


Figure 5. Left: RDFs of asphaltene–asphaltene pairs from aged, TG13-modified, and TG22-modified asphalts. Right: RDFs of asphaltene–asphaltene pairs from aged, FFA13-modified, and FFA22-modified asphalts. The x-axis denotes the inter-particle distance. The units for this measurement are given in angstroms (Å), where one angstrom is equivalent to 0.1 nanometer (nm).

The RDFs of asphaltenes with resin, aromatic, and saturate pairs are shown in Figures 6 and 7. From the RDF results of aged asphalt (solid black), the peaks existing in the RDFs of asphaltene–resin and asphaltene–aromatic pairs indicate the preferential interactions and molecular aggregations also exist between asphaltenes with aromatics and resins, but they are smaller than those between asphaltenes and asphaltenes. We believe this is because the polarities of aromatics and resins are smaller than that of asphaltenes. In addition, there is no preferential interaction observed between asphaltenes and saturates because saturates comprise the non-polar fraction in aged asphalt. Similar RDF results for asphaltene–resin, asphaltene–aromatic, and asphaltene–saturate pairs of aged asphalt were previously reported by Lemarchand et al. [58] as well. By introducing the TGs and FFAs into aged asphalt, the preferential interactions and molecular aggregations between asphaltenes with resins and aromatics are slightly reduced because the peaks of their RDFs decreased in general. This reduction in molecular aggregations between asphaltenes and resins and aromatics could contribute to the overall viscosity decrease of aged asphalt, but it would be very small. Unlike the interactions between asphaltenes and aromatic and resins, the interactions between asphaltenes and saturates remain the same even with additional WCOs.

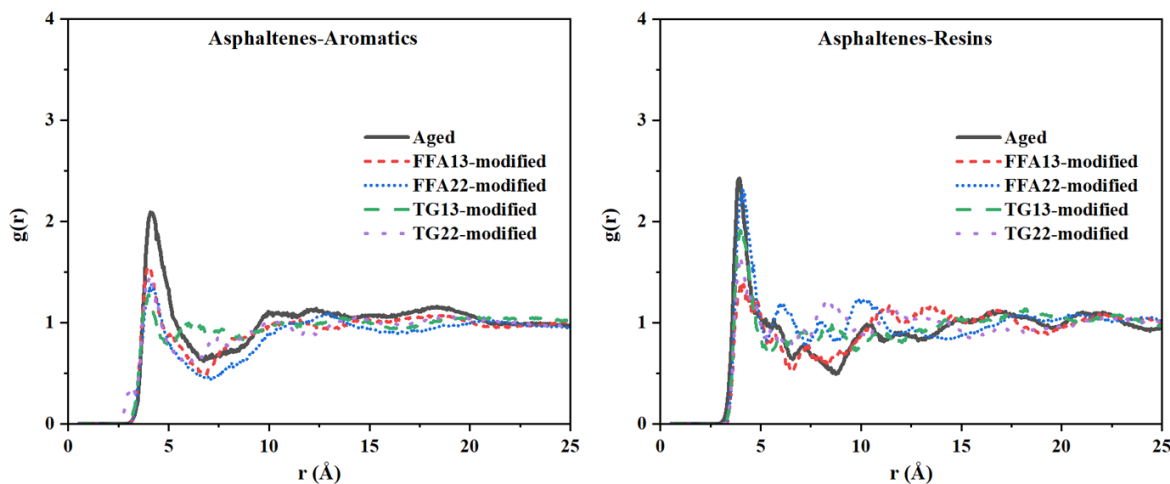


Figure 6. Left: RDFs of asphaltene–aromatic pairs of aged and WCO-modified asphalts. Right: RDFs of asphaltene–resin pairs of aged and WCO-modified asphalts.

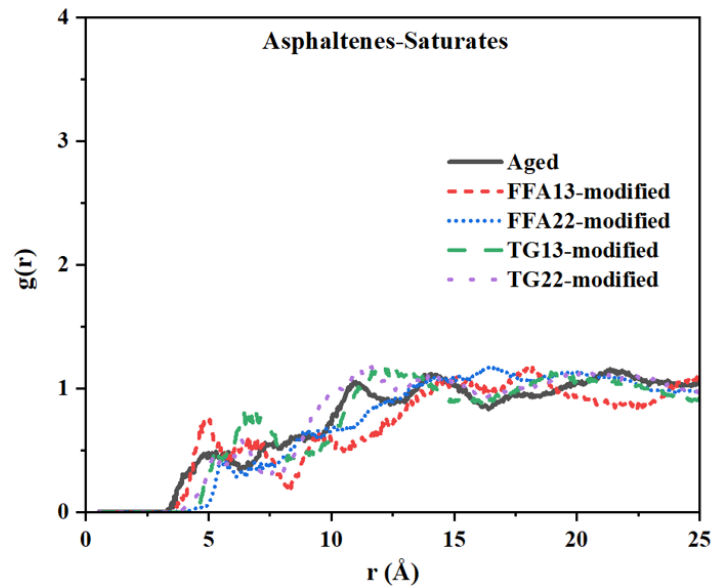


Figure 7. RDFs of asphaltene–saturate pairs of aged and WCO-modified asphalts.

3.3. Mean Square Displacement and Self-Diffusion Coefficient

The mean square displacement (MSD) measures the deviation in a particle’s position toward a reference position over time, and its generic formula is described as follows [16,60]:

$$MSD(t) = \langle |r_i(t) - r_i(0)|^2 \rangle \tag{3}$$

where $r_i(t)$ is the position of a particle i at a time t , $r_i(0)$ is the position of the particle i at the initial time ($t = 0$), and the angular bracket represents the ensemble average. The self-diffusion coefficient with Fickian diffusion relates to the MSD as follows [60]:

$$D = \lim_{t \rightarrow \infty} \frac{1}{6t} MSD(t) \tag{4}$$

where D represents the self-diffusion coefficient that is commonly used as an indication of molecular translation mobility.

The MSDs and self-diffusion coefficients of aged and WCO-modified asphalts are shown in Figure 8. Before introducing the WCOs, the aged asphalt with the largest viscosity had the smallest self-diffusion coefficient and mobility. After introducing the WCOs, all four WCOs increased the self-diffusion coefficient and mobility of the aged asphalt due to their softening effect. Furthermore, the self-diffusion coefficients of the FFA-modified asphalts are larger than those of the TG-modified asphalts, indicating that the FFA could increase the mobility of aged asphalt more efficiently than TG. Moreover, with the consideration of chain length, the FFAs and TGs with short chain lengths could increase the mobility of aged asphalt more than FFAs and TGs with long chain lengths. The observation of the MSDs and self-diffusion coefficients of aged and WCO-modified asphalts is consistent with the viscosity analysis in Section 3.1.

Saturates represent the fraction of asphalt with the smallest MW and the largest mobility [61,62]. On the left of Figure 9, the MSDs of FFA and saturate molecules were calculated, respectively, in FFA-modified asphalts. Similarly, on the right of Figure 9, the MSDs of TG and saturate molecules were determined in TG-modified asphalts. It is clear to see that the slopes of the MSDs of FFA molecules are obviously larger than those of saturates, indicating that the mobility of FFA molecules in FFA-modified asphalts is the largest, even over saturates. On the other hand, the slopes of the MSDs of TG molecules are very similar to those of saturates, suggesting that the mobility of TG molecules is at the same level of mobility as saturates in TG-modified asphalts. Hence, it can be concluded that as the FFAs were introduced into the aged asphalt, the proportion of the highest mobility

fraction increased and distributed in the aged asphalt, which increased the mobility and decreased the viscosity of the aged asphalt. However, in TG-modified asphalts, in addition to separating the asphaltene aggregations, the addition of TGs with relatively high mobility is another reason why the viscosity and mobility of TG-modified asphalts could be affected.

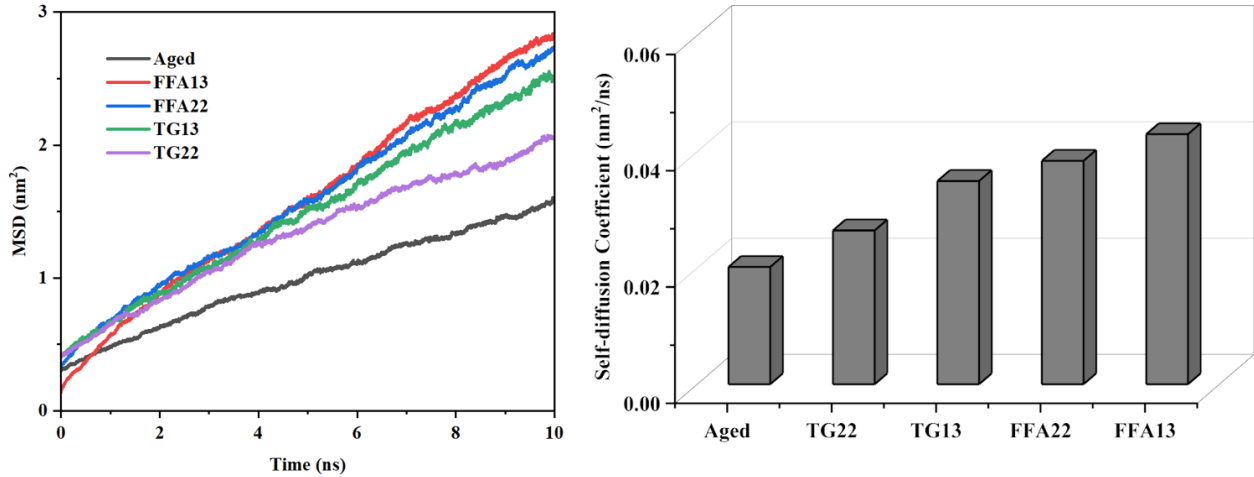


Figure 8. Left: MSDs of aged and WCO-modified asphalts. Right: Self-diffusion coefficients of aged and WCO-modified asphalts.

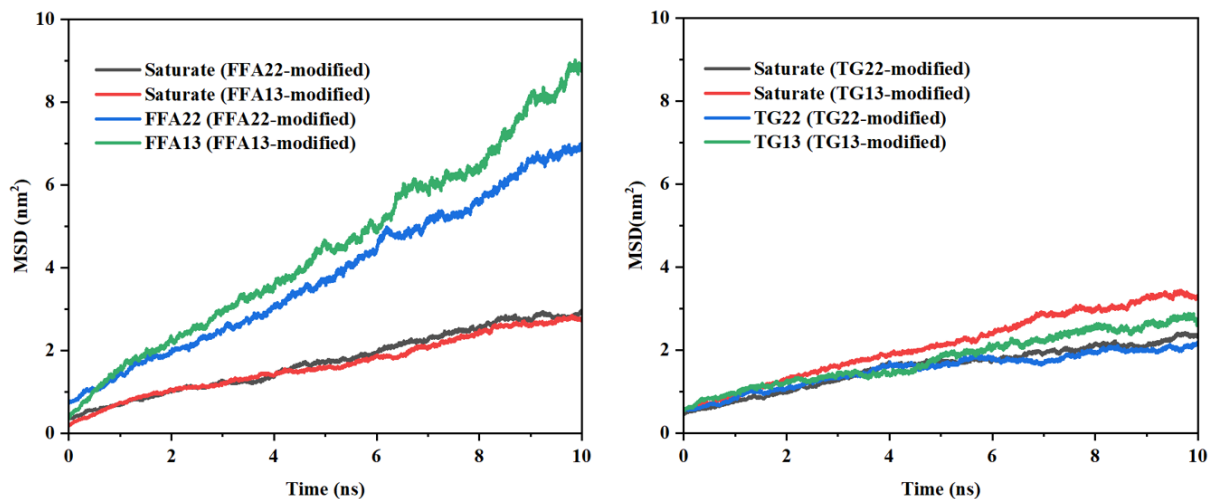


Figure 9. Left: MSDs of saturates and FFAs in FFA13-modified and FFA22-modified asphalt samples, respectively. Right: MSDs of saturates and TGs in TG13-modified and TG22-modified asphalt samples, respectively.

3.4. Chain Length Effects

In Figure 4, the result shows that the WCOs with shorter chain lengths caused better viscosity reductions in aged asphalt. The first reason is that a shorter chain length yields a smaller MW and greater translation mobility. As shown in Figure 9, both TG and FFA molecules with shorter chain lengths have greater mobility. The second reason is possibly that WCO molecules with a long chain length could entangle with other asphalt molecules heavily and affect the mobility and viscosity of the aged asphalt.

To study the entanglement of WCO molecules in modified asphalts, the method from Hsu and Violi’s paper was employed [63]. A relative distance was determined from the ratio of dt over di , where di represents the original straight distances between the first and the last carbons of FA chains, and dt represents the real distances between the first and the last carbons of FA chains when distributed in modified asphalt, as shown on the left of Figure 10. As the relative distance approaches 1, it indicates that the degree of

entanglement is small. As the relative distance approaches 0, it indicates that the degree of entanglement is large. The relative distance results of the WCOs are calculated on the right of Figure 10. Comparing TG13 with TG22 and FFA13 with FFA22, respectively, the smaller relative distances come from the longer chain lengths, which indicates that the longer chain length in the WCO would have a high probability to entangle with other asphalt molecules in modified asphalts. In Figure 11, TG13 and TG22 molecules in modified asphalts are visualized separately to support our relative distance result. It is clear that the FA chains in TG13 behave more straightly than the FA chains in TG22, which reduces their possibility of entangling with other asphalt molecules.

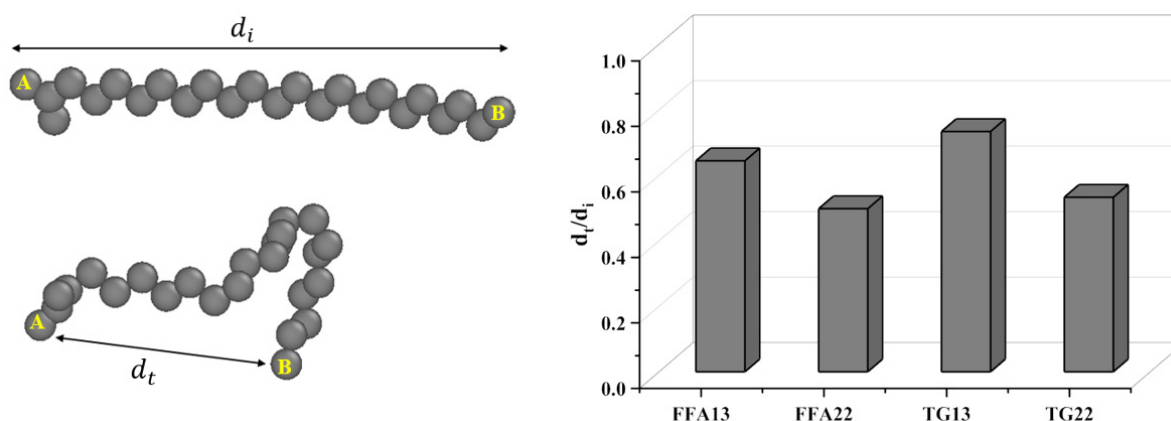


Figure 10. Left: Definition of the d_i, d_t of FFA22 molecule as an example. Right: Relative distance ratios of WCOs in modified asphalt samples.

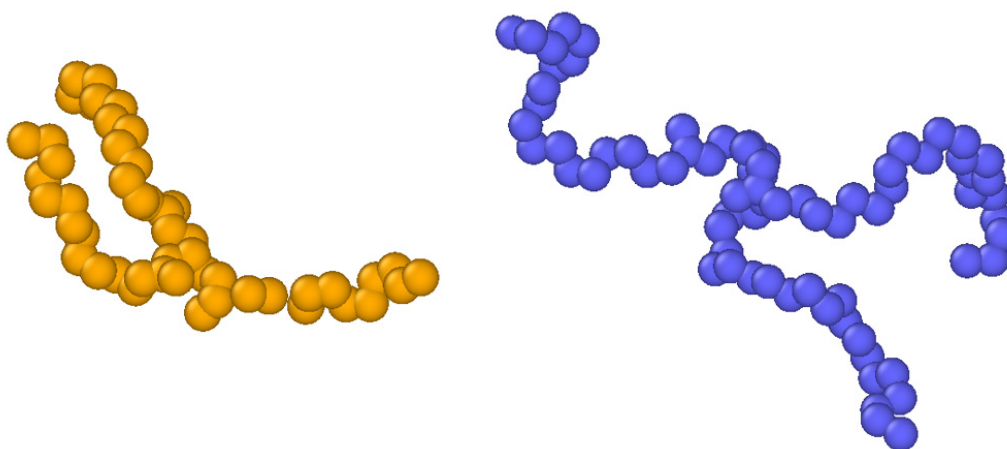


Figure 11. Orange: visualization of a TG13 molecule moving in TG13-modified asphalt. Blue: visualization of a TG22 molecule moving in TG22-modified asphalt. The asphalt molecules around the TG molecules are hidden for clarity.

In general, the large degree of entanglements between TG22 and FFA22 with other asphalt molecules would decrease the mobility of the asphalt molecules and themselves, meanwhile weakening their viscosity-reducing effect on aged asphalts compared with TG13 and FFA13, which is consistent with the viscosities and self-diffusion coefficients shown in Figures 4 and 8. In more detail, although both TG13 and TG22 could weaken the preferential interaction between asphaltenes (Figure 5) and decrease the viscosity of aged asphalt, the longer FA chains in TG22 with a higher probability of entangling with asphaltenes were likely the reason why TG22 had a smaller reducing effect on asphaltene–asphaltene interactions, as shown in Figure 5, and the viscosity of the aged asphalt compared with TG13, as shown in Figure 4. Figure 10 shows that FFA22 has a higher probability than FFA13 to entangle with other asphalt molecules. However, differences in viscosity between

FFA22-modified and FFA13-modified asphalt exist but are small, as shown in Figure 4. This is reasonable because an FFA likes a single-chain molecule with a small MW and large mobility; even if momentarily involved in a heavy entanglement, it could still be released from the entanglement easily compared with a TG. This is the reason why the effects of the chain length and molecular entanglement of an FFA on asphalt viscosity are small.

3.5. Discussions on Needed Future Experiments

The correspondence between molecular dynamics simulations and physical tests lies in the ability of simulations to predict the macroscopic properties of materials from their molecular interactions. In this study, the computed properties from MD simulations, such as viscosity and self-diffusion coefficients, were directly linked to the material's performance characteristics that can be measured in physical tests, such as penetration grade and softening point. We expect that future experimental measurements of aged and rejuvenated asphalt properties can validate our simulations. In addition, recognizing that MD simulations may not capture all the complexities of a material's behavior under varied physical conditions, we took steps to use well-established force fields and simulation parameters that were validated in previous studies.

Furthermore, we acknowledge that MD simulations serve as a complementary tool rather than a complete substitute for physical testing. They provide valuable insights into the molecular-level mechanisms that underpin the material properties observed in laboratory tests. These insights can guide the design of more effective rejuvenators and help interpret experimental results, particularly for phenomena that are difficult to measure directly or require destructive testing methods. By integrating MD simulation data with experimental findings, a more comprehensive understanding of material behavior could be achieved, allowing for the advancement of asphalt technology with predictive capabilities that reduce the time and costs associated with extensive physical testing.

We also recognize that the current understanding of the impact of waste cooking oil (WCO) on the physical–chemical properties of asphalt binders is limited. Our study addresses this knowledge gap by employing molecular dynamics simulations to elucidate the molecular interactions and changes in physical properties when WCO is introduced into aged asphalt binders.

The novel contribution of our research lies in the detailed analysis of the molecular structure of WCO and its interaction with asphalt components. We investigated how different constituents of WCO, such as triglycerides and free fatty acids, influence the microstructure and rheological properties of asphalt, which are indicative of its macroscopic behavior. Additionally, our work explores the potential of WCO as a sustainable rejuvenator by providing a deeper understanding of its mechanisms of action at the molecular level. This can pave the way for future empirical studies and the development of new, environmentally friendly methods for asphalt pavement restoration.

To further the field's knowledge base, we propose additional experimental studies to validate and complement our simulation results. We also encourage the asphalt research community to explore the long-term performance and durability of WCO-modified asphalt binders through physical aging and performance tests.

4. Conclusions

In this study, molecular dynamics simulations were conducted to assess the impact of triglycerides (TGs) and free fatty acids (FFAs), core components of waste cooking oil, on the viscosity, self-diffusion, and microstructure of aged asphalt. The results demonstrated that both FFAs and TGs significantly reduce the viscosity of aged asphalt, lowering it from 12 cP to approximately 6 cP and 8 cP, respectively. However, the underlying modification mechanisms were found to differ, as revealed by microstructure and self-diffusion analyses. With radial distribution functions to investigate the microstructure of aged and TG-modified asphalts, it became apparent that TG played a crucial role in weakening the preferential interactions among asphaltenes and mitigating the self-aggregations formed by these

molecules. This disruption of asphaltene interactions significantly contributed to the viscosity reduction observed in the aged asphalt. In contrast, in FFA-modified asphalts, these preferential interactions between asphaltenes remained largely unaltered. An analysis of mean square displacements and self-diffusion coefficients revealed that TGs exhibited similar self-diffusion coefficients to saturates. This finding suggested that the increase in components with greater mobility within aged asphalt was another factor contributing to the viscosity reduction when TG was introduced. In the case of FFA-modified asphalt, the FFA displayed the highest self-diffusion coefficient, surpassing even that of saturates. Consequently, it was inferred that the elevated proportion of highly mobile components, such as the FFA fraction, was the primary driver behind the viscosity reduction in FFA-modified aged asphalt. Furthermore, the study investigated the entanglement behavior of fatty acid (FA) chains with varying lengths. It was observed that when compared to longer chain lengths, WCO molecules with shorter chain lengths had a lower likelihood of entanglement with other asphalt molecules. This property resulted in increased molecular mobility and a subsequent reduction in the viscosity of aged asphalt. These insights provide a comprehensive understanding of the molecular dynamics underpinning the effects of TGs and FFAs on the properties of aged asphalt.

Author Contributions: Conceptualization, methodology, software, formal analysis, investigation, data curation, and writing—original draft preparation: Q.C.; conceptualization, methodology, investigation, and writing—review and editing: L.H.; software and formal analysis: Y.W. All authors have read and agreed to the published version of the manuscript.

Funding: This research received no external funding.

Data Availability Statement: Data will be made available upon request.

Acknowledgments: We acknowledge the Supercomputing Center for Education & Research (OSCER) at the University of Oklahoma and the Department of Civil and Natural Resources Engineering at the University of Canterbury for computational resources and dedicated support.

Conflicts of Interest: The authors declare no conflict of interest.

Abbreviations

FFA	Free fatty acid
FA	Fatty acid
LAMMPS	Large-scale atomic/molecular massively parallel simulator
MD	Molecular dynamics
MW	Molecular weight
MSD	Mean square displacement
NVT	Canonical ensemble
NPT	Isothermal-isobaric ensemble
OPLS-AA	Optimized potentials for liquid simulations—all atom
PPPM	Particle–particle–particle–mesh
P/T	Pressure and temperature
RDF	Radial distribution function
SARA	Saturates, aromatics, resins, asphaltenes
TG	Triglyceride
WCO	Waste cooking oil
WCOs	Waste cooking oils
WVO	Waste vegetable oil
WVOs	Waste vegetable oils

References

1. George, A.M.; Banerjee, A.; Puppala, A.J.; Saladhi, M. Performance evaluation of geocell-reinforced reclaimed asphalt pavement (RAP) bases in flexible pavements. *Int. J. Pavement Eng.* **2021**, *22*, 181–191. [[CrossRef](#)]
2. Li, H.; Dong, B.; Wang, W.; Zhao, G.; Guo, P.; Ma, Q. Effect of waste engine oil and waste cooking oil on performance improvement of aged asphalt. *Appl. Sci.* **2019**, *9*, 1767. [[CrossRef](#)]

3. Herrington, P.R.; Patrick, J.E.; Ball, G.F. Oxidation of roading asphalts. *Ind. Eng. Chem. Res.* **1994**, *33*, 2801–2809. [[CrossRef](#)]
4. Petersen, J.C.; Glaser, R. Asphalt oxidation mechanisms and the role of oxidation products on age hardening revisited. *Road Mater. Pavement Des.* **2011**, *12*, 795–819. [[CrossRef](#)]
5. Traxler, R. Relation between Asphalt Composition and Hardening by Volatilization and Oxidation. *Assoc. Asphalt Paving Technol. Proc.* **1961**, *30*, 359–372.
6. Pan, J.; Tarefder, R.A. Investigation of asphalt aging behaviour due to oxidation using molecular dynamics simulation. *Mol. Simul.* **2016**, *42*, 667–678. [[CrossRef](#)]
7. Elahi, Z.; Mohd Jakarni, F.; Muniandy, R.; Hassim, S.; Ab Razak, M.S.; Ansari, A.H.; Ben Zair, M.M. Waste cooking oil as a sustainable bio modifier for asphalt modification: A review. *Sustainability* **2021**, *13*, 11506. [[CrossRef](#)]
8. Luo, Y.; Zhang, K. Review on performance of asphalt and asphalt mixture with waste cooking oil. *Materials* **2023**, *16*, 1341. [[CrossRef](#)] [[PubMed](#)]
9. Zargar, M.; Ahmadiania, E.; Asli, H.; Karim, M.R. Investigation of the possibility of using waste cooking oil as a rejuvenating agent for aged bitumen. *J. Hazard. Mater.* **2012**, *233*, 254–258. [[CrossRef](#)] [[PubMed](#)]
10. Ji, J.; Yao, H.; Suo, Z.; You, Z.; Li, H.; Xu, S.; Sun, L. Effectiveness of vegetable oils as rejuvenators for aged asphalt binders. *J. Mater. Civ. Eng.* **2017**, *29*, D4016003. [[CrossRef](#)]
11. Cao, X.; Wang, H.; Cao, X.; Sun, W.; Zhu, H.; Tang, B. Investigation of rheological and chemical properties asphalt binder rejuvenated with waste vegetable oil. *Constr. Build. Mater.* **2018**, *180*, 455–463. [[CrossRef](#)]
12. Gökalp, İ.; Uz, V.E. Utilizing of Waste Vegetable Cooking Oil in bitumen: Zero tolerance aging approach. *Constr. Build. Mater.* **2019**, *227*, 116695. [[CrossRef](#)]
13. Sonibare, K.; Rucker, G.; Zhang, L. Molecular dynamics simulation on vegetable oil modified model asphalt. *Constr. Build. Mater.* **2021**, *270*, 121687. [[CrossRef](#)]
14. Li, L.; Xin, C.; Guan, M.; Guo, M. Using molecular dynamics simulation to analyze the feasibility of using waste cooking oil as an alternative rejuvenator for aged asphalt. *Sustainability* **2021**, *13*, 4373. [[CrossRef](#)]
15. Qu, X.; Liu, Q.; Wang, C.; Wang, D.; Oeser, M. Effect of co-production of renewable biomaterials on the performance of asphalt binder in macro and micro perspectives. *Materials* **2018**, *11*, 244. [[CrossRef](#)] [[PubMed](#)]
16. Chang, Q.; Edgar, A., III; Ghos, S.; Zaman, M.; Huang, L.; Wu, X. An atomistic model of aged asphalt guided by the oxidation chemistry of benzylic carbon with application to asphalt rejuvenated with a triglyceride. *Constr. Build. Mater.* **2023**, *400*, 132743. [[CrossRef](#)]
17. Xu, N.; Wang, H.; Wang, H.; Kazemi, M.; Fini, E. Research progress on resource utilization of waste cooking oil in asphalt materials: A state-of-the-art review. *J. Clean. Prod.* **2022**, *385*, 135427. [[CrossRef](#)]
18. Cárdenas, J.; Orjuela, A.; Sánchez, D.L.; Narváez, P.C.; Katryniok, B.; Clark, J. Pre-treatment of used cooking oils for the production of green chemicals: A review. *J. Clean. Prod.* **2021**, *289*, 125129. [[CrossRef](#)]
19. Raclot, T.; Groscolas, R. Differential mobilization of white adipose tissue fatty acids according to chain length, unsaturation, and positional isomerism. *J. Lipid Res.* **1993**, *34*, 1515–1526. [[CrossRef](#)]
20. Brodholt, J.; Wood, B. Molecular dynamics of water at high temperatures and pressures. *Geochim. Cosmochim. Acta* **1990**, *54*, 2611–2616. [[CrossRef](#)]
21. Zhou, Y.; Huang, J.; Yang, X.; Dong, Y.; Feng, T.; Liu, J. Enhancing the PVA fiber-matrix interface properties in ultra high performance concrete: An experimental and molecular dynamics study. *Constr. Build. Mater.* **2021**, *285*, 122862. [[CrossRef](#)]
22. Jin, L.; He, Y.; Zhou, G.; Chang, Q.; Huang, L.; Wu, X. Natural gas density under extremely high pressure and high temperature: Comparison of molecular dynamics simulation with corresponding state model. *Chin. J. Chem. Eng.* **2021**, *31*, 2–9. [[CrossRef](#)]
23. Chen, F.; Yang, R.; Wang, Z.; Zhang, G.; Yu, R. Rheological analysis and molecular dynamics modeling of Ultra-High Performance Concrete for wet-mix spraying. *J. Build. Eng.* **2023**, *68*, 106167. [[CrossRef](#)]
24. Liu, X.; Zhang, D. A review of phase behavior simulation of hydrocarbons in confined space: Implications for shale oil and shale gas. *J. Nat. Gas Sci. Eng.* **2019**, *68*, 102901. [[CrossRef](#)]
25. Chang, Q.; Huang, L.; Wu, X. Combination of simplified local density theory and molecular dynamics simulation to study the local density distribution of hydrocarbon gas in shale gas reservoir. In Proceedings of the SPE Eastern Regional Meeting, Charleston, WV, USA, 15–17 October 2019; p. D022S005R006.
26. Foroutan, M.; Fatemi, S.M.; Esmaeilian, F. A review of the structure and dynamics of nanoconfined water and ionic liquids via molecular dynamics simulation. *Eur. Phys. J. E* **2017**, *40*, 1–14. [[CrossRef](#)]
27. Liu, J.; Wu, Y.; Shen, J.; Gao, Y.; Zhang, L.; Cao, D. Polymer–nanoparticle interfacial behavior revisited: A molecular dynamics study. *Phys. Chem. Chem. Phys.* **2011**, *13*, 13058–13069. [[CrossRef](#)]
28. Yang, Y.; Nair, A.K.N.; Ruslan, M.F.A.C.; Sun, S. Interfacial properties of the aromatic hydrocarbon+ water system in the presence of hydrophilic silica. *J. Mol. Liq.* **2022**, *346*, 118272. [[CrossRef](#)]
29. Chang, Q.; Huang, L.; Wu, X. A Molecular Dynamics Study on Low-Pressure Carbon Dioxide in the Water/Oil Interface for Enhanced Oil Recovery. *SPE J.* **2023**, *28*, 643–652. [[CrossRef](#)]
30. Tien, C.-L.; Weng, J.-G. Molecular dynamics simulation of nanoscale interfacial phenomena in fluids. *Adv. Appl. Mech.* **2002**, *38*, 95–146.
31. Hollingsworth, S.A.; Dror, R.O. Molecular dynamics simulation for all. *Neuron* **2018**, *99*, 1129–1143. [[CrossRef](#)]

32. Perilla, J.R.; Goh, B.C.; Cassidy, C.K.; Liu, B.; Bernardi, R.C.; Rudack, T.; Yu, H.; Wu, Z.; Schulten, K. Molecular dynamics simulations of large macromolecular complexes. *Curr. Opin. Struct. Biol.* **2015**, *31*, 64–74. [[CrossRef](#)] [[PubMed](#)]
33. Rapaport, D.C. *The Art of Molecular Dynamics Simulation*; Cambridge University Press: Cambridge, UK, 2004.
34. Chen, Z.; Pei, J.; Li, R.; Xiao, F. Performance characteristics of asphalt materials based on molecular dynamics simulation—A review. *Constr. Build. Mater.* **2018**, *189*, 695–710. [[CrossRef](#)]
35. Yao, H.; Liu, J.; Xu, M.; Ji, J.; Dai, Q.; You, Z. Discussion on molecular dynamics (MD) simulations of the asphalt materials. *Adv. Colloid Interface Sci.* **2022**, *299*, 102565. [[CrossRef](#)] [[PubMed](#)]
36. Corbett, L.W. Composition of asphalt based on generic fractionation, using solvent deasphalting, elution-adsorption chromatography, and densimetric characterization. *Anal. Chem.* **1969**, *41*, 576–579. [[CrossRef](#)]
37. Zhang, L.; Greenfield, M.L. Molecular orientation in model asphalts using molecular simulation. *Energy Fuels* **2007**, *21*, 1102–1111. [[CrossRef](#)]
38. Li, D.D.; Greenfield, M.L. Chemical compositions of improved model asphalt systems for molecular simulations. *Fuel* **2014**, *115*, 347–356. [[CrossRef](#)]
39. Wang, P.; Dong, Z.-j.; Tan, Y.-q.; Liu, Z.-y. Investigating the interactions of the saturate, aromatic, resin, and asphaltene four fractions in asphalt binders by molecular simulations. *Energy Fuels* **2015**, *29*, 112–121. [[CrossRef](#)]
40. Petersen, J.C. A review of the fundamentals of asphalt oxidation: Chemical, physicochemical, physical property, and durability relationships. *Transp. Res. Circ.* 2009.
41. Azahar, W.N.A.W.; Jaya, R.P.; Hainin, M.R.; Bujang, M.; Ngadi, N. Chemical modification of waste cooking oil to improve the physical and rheological properties of asphalt binder. *Constr. Build. Mater.* **2016**, *126*, 218–226. [[CrossRef](#)]
42. Asli, H.; Ahmadinia, E.; Zargar, M.; Karim, M.R. Investigation on physical properties of waste cooking oil–Rejuvenated bitumen binder. *Constr. Build. Mater.* **2012**, *37*, 398–405. [[CrossRef](#)]
43. Thompson, A.P.; Aktulga, H.M.; Berger, R.; Bolintineanu, D.S.; Brown, W.M.; Crozier, P.S.; in't Veld, P.J.; Kohlmeyer, A.; Moore, S.G.; Nguyen, T.D. LAMMPS—a flexible simulation tool for particle-based materials modeling at the atomic, meso, and continuum scales. *Comput. Phys. Commun.* **2022**, *271*, 108171. [[CrossRef](#)]
44. Jorgensen, W.L.; Maxwell, D.S.; Tirado-Rives, J. Development and testing of the OPLS all-atom force field on conformational energetics and properties of organic liquids. *J. Am. Chem. Soc.* **1996**, *118*, 11225–11236. [[CrossRef](#)]
45. Jorgensen, W.L.; McDonald, N.A. Development of an all-atom force field for heterocycles. Properties of liquid pyridine and diazenes. *J. Mol. Struct. Theochem.* **1998**, *424*, 145–155. [[CrossRef](#)]
46. McDonald, N.A.; Jorgensen, W.L. Development of an all-atom force field for heterocycles. Properties of liquid pyrrole, furan, diazoles, and oxazoles. *J. Phys. Chem. B* **1998**, *102*, 8049–8059. [[CrossRef](#)]
47. Robertson, M.J.; Tirado-Rives, J.; Jorgensen, W.L. Improved peptide and protein torsional energetics with the OPLS-AA force field. *J. Chem. Theory Comput.* **2015**, *11*, 3499–3509. [[CrossRef](#)]
48. Szewczyk, P. Study of the Phase Behavior of Triacylglycerols Using Molecular Dynamics Simulation. Master's Thesis, University of Alberta, Edmonton, AB, Canada, 2010. [[CrossRef](#)]
49. Martínez, L.; Andrade, R.; Birgin, E.G.; Martínez, J.M. PACKMOL: A package for building initial configurations for molecular dynamics simulations. *J. Comput. Chem.* **2009**, *30*, 2157–2164. [[CrossRef](#)] [[PubMed](#)]
50. Xu, G.; Wang, H. Molecular dynamics study of oxidative aging effect on asphalt binder properties. *Fuel* **2017**, *188*, 1–10. [[CrossRef](#)]
51. Chang, Q.; Huang, L.; Wu, X. A Molecular-Level Study on the Interaction Behavior between Polyethylene and Aged Asphalt. In Proceedings of the International Conference on Transportation and Development, Seattle, WA, USA, 31 May–3 June 2022; pp. 179–189. Available online: <https://hdl.handle.net/11244/336908> (accessed on 4 December 2023).
52. Chang, Q. Study of Multicomponent of Hydrocarbon Systems with Molecular Dynamics Simulation. Ph.D. Thesis, University of Oklahoma, Norman, OK, USA, 2022.
53. Zhang, L.; Greenfield, M.L. Relaxation time, diffusion, and viscosity analysis of model asphalt systems using molecular simulation. *J. Chem. Phys.* **2007**, *127*, 194502. [[CrossRef](#)]
54. Vargas, M.A.; Vargas, M.A.; Sánchez-Sólis, A.; Manero, O. Asphalt/polyethylene blends: Rheological properties, microstructure and viscosity modeling. *Constr. Build. Mater.* **2013**, *45*, 243–250. [[CrossRef](#)]
55. Cui, B.; Gu, X.; Hu, D.; Dong, Q. A multiphysics evaluation of the rejuvenator effects on aged asphalt using molecular dynamics simulations. *J. Clean. Prod.* **2020**, *259*, 120629. [[CrossRef](#)]
56. Altgelt, K.; Harle, O. The effect of asphaltenes on asphalt viscosity. *Ind. Eng. Chem. Prod. Res. Dev.* **1975**, *14*, 240–246. [[CrossRef](#)]
57. Li, X.; Chi, P.; Guo, X.; Sun, Q. Effects of asphaltene concentration and asphaltene agglomeration on viscosity. *Fuel* **2019**, *255*, 115825. [[CrossRef](#)]
58. Lemarchand, C.A.; Schröder, T.B.; Dyre, J.C.; Hansen, J.S. Coee bitumen: Chemical aging. *J. Chem. Phys.* **2013**, *139*, 124506. [[CrossRef](#)]
59. Khabaz, F.; Khare, R. Glass transition and molecular mobility in styrene–butadiene rubber modified asphalt. *J. Phys. Chem. B* **2015**, *119*, 14261–14269. [[CrossRef](#)] [[PubMed](#)]
60. Heyes, D.M. Self-diffusion and shear viscosity of simple fluids. A molecular-dynamics study. *J. Chem. Soc. Faraday Trans. 2 Mol. Chem. Phys.* **1983**, *79*, 1741–1758. [[CrossRef](#)]
61. Chen, S.; Yang, Q.; Qiu, X.; Liu, K.; Xiao, S.; Xu, W. Use of MD Simulation for Investigating Diffusion Behaviors between Virgin Asphalt and Recycled Asphalt Mastic. *Buildings* **2023**, *13*, 862. [[CrossRef](#)]

62. Du, Z.; Zhu, X. Molecular dynamics simulation to investigate the adhesion and diffusion of asphalt binder on aggregate surfaces. *Transp. Res. Rec.* **2019**, *2673*, 500–512. [[CrossRef](#)]
63. Hsu, W.-D.; Violi, A. Order—Disorder phase transformation of triacylglycerols: Effect of the structure of the aliphatic chains. *J. Phys. Chem. B* **2009**, *113*, 887–893. [[CrossRef](#)]

Disclaimer/Publisher’s Note: The statements, opinions and data contained in all publications are solely those of the individual author(s) and contributor(s) and not of MDPI and/or the editor(s). MDPI and/or the editor(s) disclaim responsibility for any injury to people or property resulting from any ideas, methods, instructions or products referred to in the content.